Fracture Mechanics of Concrete Structures
Proceedings FRAMCOS-3
AEDIFICATIO Publishers, D-79104 Freiburg, Germany

FINITE ELEMENT ANALYSIS OF THERMAL CRACK IN GRAVITY DAM CAUSED BY ANNUALLY OSCILLATING ENVIRONMENTAL TEMPERATURE

M. Irobe
Tokyo, Japan
S.Y. Peng
Engineering Department, Miura Boiler co., Ontario, Canada

Abstract

This paper describes the development of thermal cracks in a gravity dam caused by idealized annual temperature change of the dam concrete. Crack occurs across the layer of concrete along the down stream surface due to the severe thermal gradient during the descending process of temperature. Crack line is assumed to develop on an inter-boundary of finite elements so that a particular remeshing technique is not used. Crack closes as the surface temperature gets near the lowest. Link element is put between the nodes pair on the crack surfaces when the space becomes narrower than a certain limit. Time and place of thermal cracking and variations of stress intensity factors during one cycle of the annual temperature change are discussed.
Key words: Cracking, cyclic thermal load, heat conduction, stress intensity factors

1 Introduction

Two kinds of causes can be mentioned for occurrence of thermal crack in massive concrete structures such as the gravity dam. One is the thermal shrinkage of concrete

due to the radiation and diffusion of the cement hydration heat. The other is the difference of volume changes in a concrete layer near surface according to the thermal gradient caused by the seasonal environmental temperature change. Higashigawa et al. (1992) and Noike et al. (1994) analyzed thermal stresses in a gravity dam to predict the thermal cracks due to the latter cause. Okubo et al. (1989) analyzed the thermal cracks in massive concrete layers due to the former cause. Using the interface element which yields in tensile region, they met with success to investigate generating, opening, and closing of the crack. They named the interface element as gap element. They observed in field tests that the space of thermal cracks which initiated from the free surface of massive concrete layer was from 2.0 m to 5.0 m and a few of these surface cracks grew to structural cracks with 10.0 m to 20.0 m gap. Shimizu et al. (1989) presented a very suggestive numerical investigation on the time-dependent behavior of the surface crack in a massive concrete block. They analyzed discrepancies between two cases of crack behaviors over 60 days. The temperature drops during the period were assumed as 30℃ in one case and 15℃ in the other.

Based upon the observation of Okubo et al. (1989), in this paper let the size of the finite elements along the down stream surface be 2.5 m long and 1.5 m wide. We assume that inter-boundaries of these elements which intersect the down stream surface at right angle form the thermal cracks. Because the thermal fracture discussed in this paper is eventually the consequence of the shrinkage of concrete, the crack initiation is defined by the maximum principal stress theory. We do not use the "embedded" gap element. We made the crack surfaces free by releasing the nodal forces pair at the instant of crack opening, and gave the nodes pair some restraining by the "interfacial" link element for the crack closing less than a certain limit angle. Non-linearity was given the link element. The link elements were effective to investigate behaviors of cracks including variations of stress intensity factors (SIFs). The nodal forces pair are calculated by the simple way, i.e. the numerical integration of the stresses at Gauss points in the fracture element. It is notable that fairly high SIFs at thermal crack tips in the middle height of dam were obtained in cold season.

2 Temperature changes in dam concrete and foundation rock

The shape of dam and rock foundation, and the element discretization pattern are shown in Fig.1. The nine nodes quadrilateral isoparametric element is used. Thermal properties of dam concrete and foundation rock are presented together with mechanical ones in Table 1. Annual temperature changes of upstream and downstream surfaces of the dam are simplified by sinusoidal functions with a period of one year, so the temperatures of concrete and rock change sinusoidally as time-temperature curves shown in Fig.2.

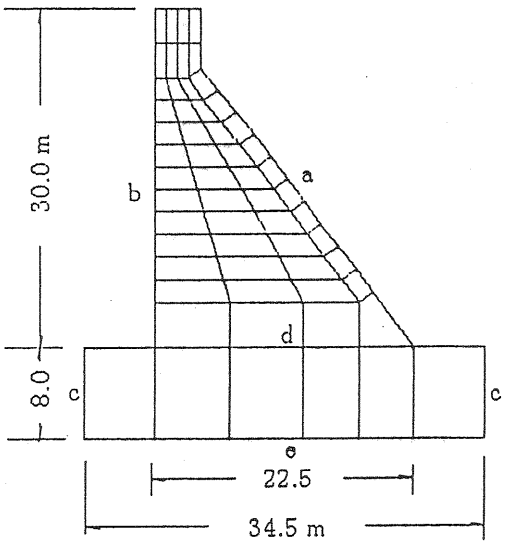

a: downstream surface, conductive boundary
b: upstream surface, conductive boundary
c: downstream and upstream edges of rock foundation, adiabatic boundary
d: contact boundary of concrete to rock
e: constant temperature (16℃) boundary

Fig.1 Shape of dam and finite element pattern

Table 1 Material constants of concrete and rock

	thermal diffusivity	Young's modulus	Poisson's ratio
concrete	0.096 (m^2/day)	32 GPa (at 20℃)	0.2
rock	0.075 (m^2/day)	11 GPa	0.2

Curves are obtained under the condition of the initial temperature 16℃ for concrete and rock. Number of the curve means nodal point shown in the attached figure.

Owing to air movement and solar radiation on the downstream surface, and inflow, outflow and convection of reservoir water on the upstream surface, temperature of the dam surface is generally very complicated. In this analysis, however, it is simply defined as curves 12 for downstream, and 1, 2 and 3 for upstream surfaces respectively.

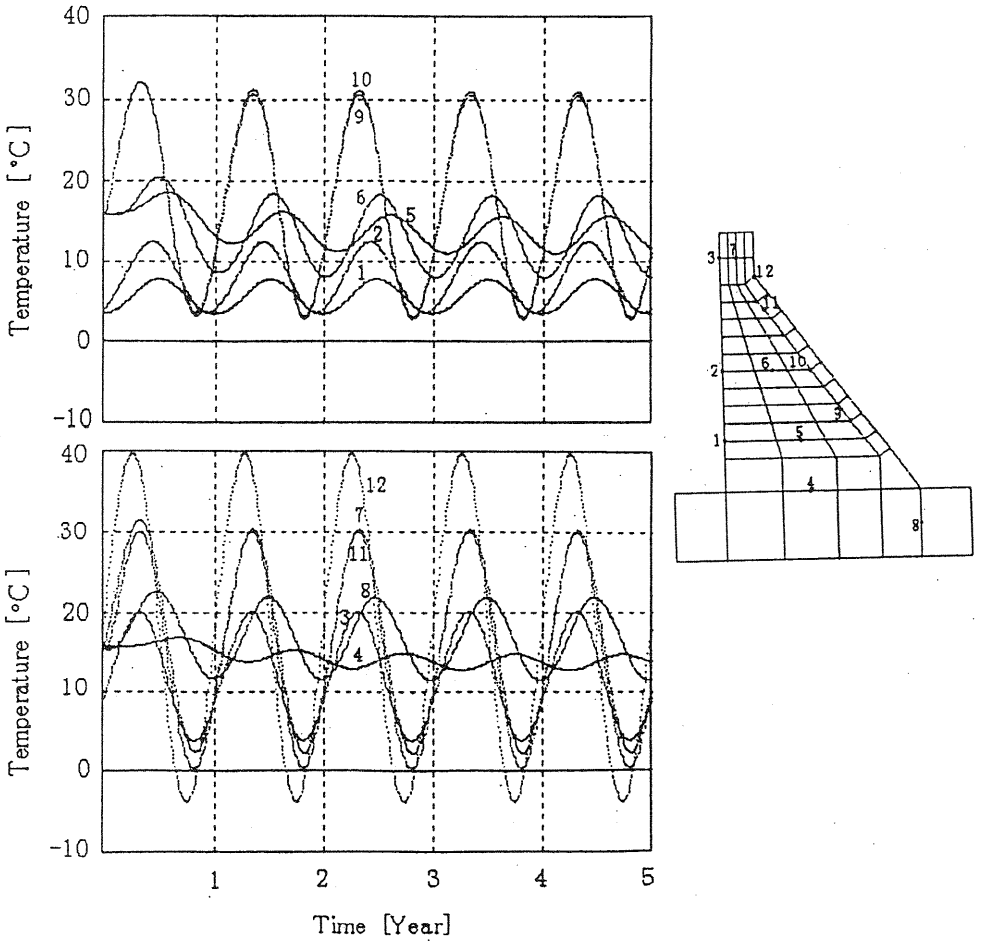

Fig. 2 Time-temperature curves of concrete and foundation rock

Using the same finite elements failure analysis in the following section are performed for the temperature of the 5th year because of its steadiness.

3 Thermal crack analysis

3.1 Initial stress

It is also complicated to determine the actual initial stress state of concrete dam. It is governed by the sequence of concrete placing, the effect of cement hydration heat, the maturity of concrete, and so on.

In this investigation these time dependent problems were disregarded, and the initial stresses at $t = 0$ are obtained by unreal loads acting instantaneously to the dam after

completion of the maturity. Loads of three kinds, i.e. own weight, water pressure on the upstream surface, and pore pressure in concrete, are taken into account.

3.2 Combined stress

Combined stresses are calculated every time step Δt as follows.

$$\sigma(t+\Delta t) = \sigma(t) + \Delta\sigma(t+\Delta t, \theta, \Delta\theta) \qquad (1)$$

where $\sigma(t+\Delta t)$ is the combined stress of the current initial stress $\sigma(t)$ and incremental thermal stress $\Delta\sigma$. Young's modulus of concrete depends upon the temperature. The incremental thermal stress is, therefore, expressed as a function of current temperature θ. Various expressions for temperature-dependent E_θ are given by several investigators. Following expression by Bangash (1989) is used to calculate the incremental stress $\Delta\sigma$.

$$E_\theta = E_{20}\left(1 - \frac{\theta - 20}{137}\right) \qquad (2)$$

He suggested that the effective range of Eq. 2 is from 20℃ to 50℃. However, we extended expediently the range from −4℃ to 50℃.

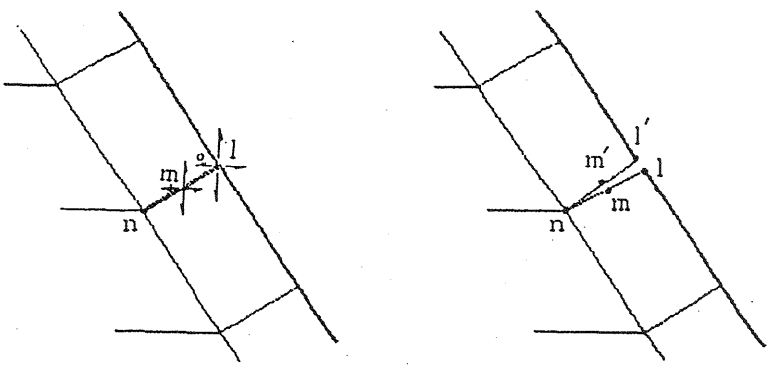

(a) Before cracking (b) After cracking

∘ Gauss point in critical condition

• Nodal points on free edges

Fig. 3 Before and after thermal crack initiation from downstream surface

We have no experimental data on criterion for the thermal crack initiation. For simplicity we used, therefore, the maximum principal stress theory, and assumed 3.5 N/mm^2 for the stress limit. The closest inter-boundary across the down stream surface

to a Gauss point where the maximum principal stress reaches the stress limit is assumed to form a crack line. The inter-boundary changes to two free edges of elements. It can be realized numerically by making nodes on the inter-boundary double nodes, and applying nodal loads with equal magnitude and opposite sign to nodal forces to the double nodes, as shown in Fig. 3.

Daily changes of the maximum principal stresses were computed for the last 5th year. Time-stress curves of several points are shown in Fig.4. Number of the curve means Gauss point shown in the attached figure. Remarkable jump and drop of the stress except point 1 are observed. It is the result of stress redistribution.

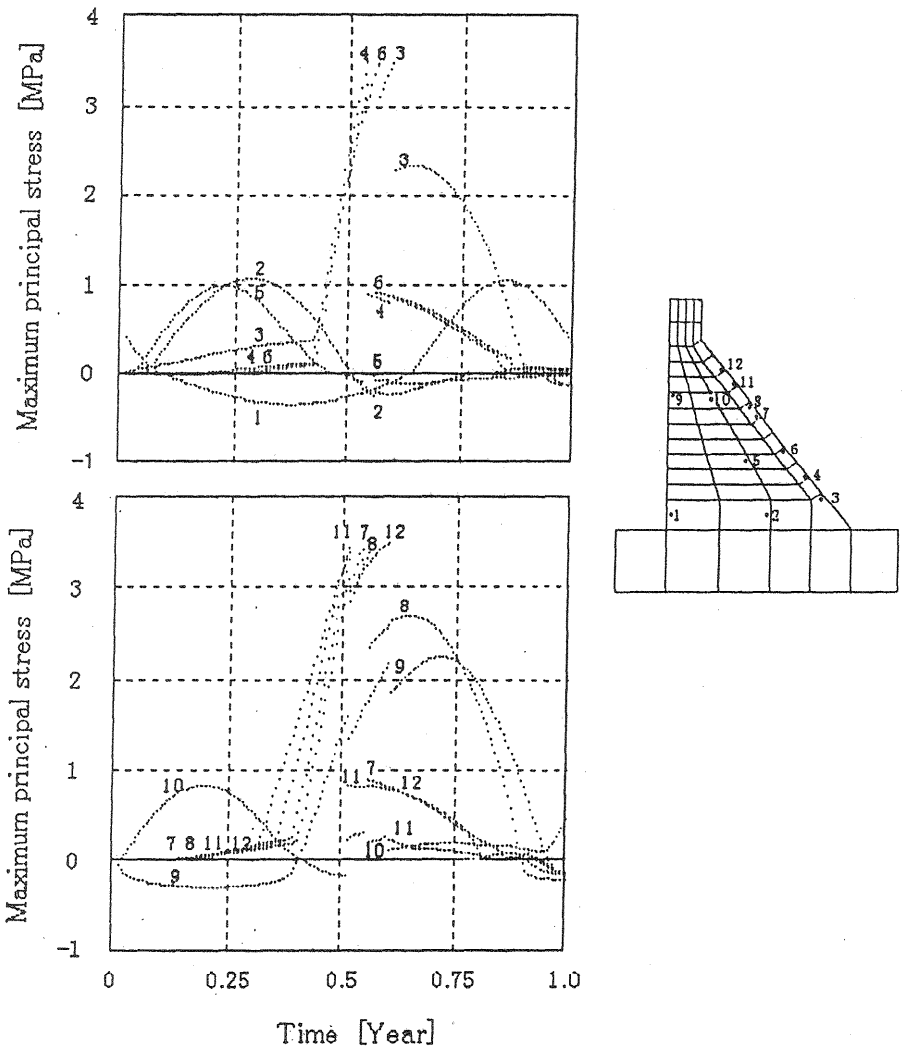

Fig.4 Time-maximum principal stress curve affected by thermal cracks

Curves for points near the down stream surface have a sharp bend. It is due to the rotation of the principal axis arising from the change of sign of the thermal gradient.

3.3 Behavior of thermal crack

Numerical results show that the crack begins to close, after the concrete temperature on the crack surface goes down lower than its initial temperature in descending branch of the time-temperature curve.

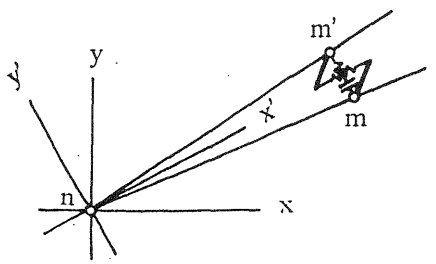

Fig.5 Nonlinear interfacial link element connecting nodes pair

We assume that if crack opening angle becomes smaller than a certain limit, a resistance to contact starts to work between the nodes pair. The limits were specified as $0.36 \cdot 10^{-3}$ rad for inner and $0.18 \cdot 10^{-3}$ rad for outer nodes pairs. The resistance was represented by interfacial link element which consists of two nonlinear springs against closing and sliding as shown in Fig.5. It is similar to the link element proposed by Scordelis (1974). The initial stiffness was determined from the relation of nodal displacements to the nodal loads for the release of nodal forces. For the final stiffness enough large quantity corresponding to infinity was given. The intermediate stiffness was assumed to increase linearly.

Fig.6 (a) shows variations of the crack opening angles obtained under these assumptions. The angle in the figure is a vertical angle at a crack tip to inner nodes pair. The date and the sequence of crack generation are presented in Fig.6 (b).

The first thermal crack generates at the 185th day and its opening angle is $0.412 \cdot 10^{-3}$ rad. It increases gradually till the 198th day, and then decreases abruptly in consequence of generation of the lower neighboring crack 3. Similar movement of crack 1 is observed around the 217th day. It is a result of generation of the immediate upper neighboring crack 6. Maximum of the opening angle of crack 1 appears at the 217th day (0.6 year). It is $0.572 \cdot 10^{-3}$ rad.

Generation of crack 2 has no effect on the behavior of crack 1. In comparison with changes of stresses, crack opening angles are insensitive to the other crack ups and downs. It is remarkable that cracks concentrate in the upper and lower parts of dam.

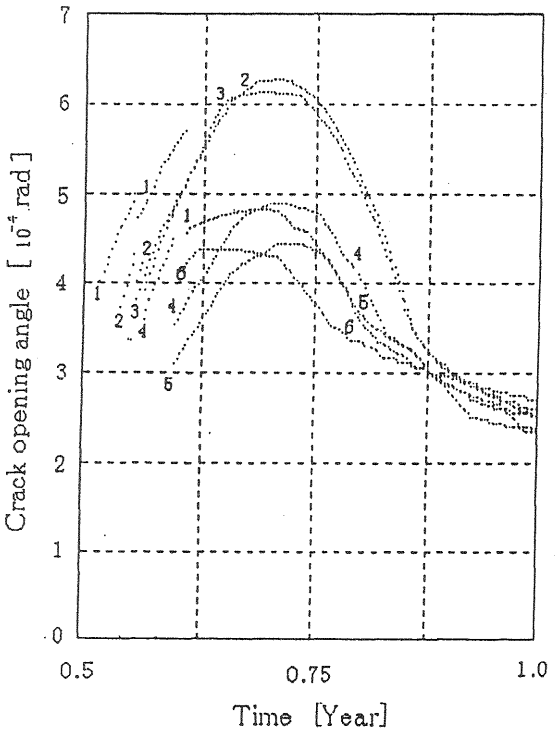

(a) Time-crack opening angle curve

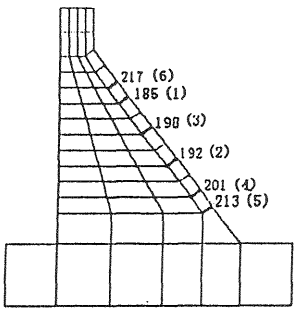

(b) Time (day) and place of crack (bold line) generation

Fig.6 Time-crack opening angle curve of thermal crack on down stream surface

3.4 Stress intensity factors at thermal crack tips

Using the following expression SIFs are obtained with the local coordinate system shown in Fig. 5. Taking coordinates of nodes m and m' at the moment of the crack generation as their initial coordinates, nodal displacements are determined day by day.

$$K_I(t) = \frac{G}{(\kappa+1)}\sqrt{\frac{2\pi}{r}}(v_{m'}(t) - v_m(t))$$

$$K_{II}(t) = \frac{G}{(\kappa+1)}\sqrt{\frac{2\pi}{r}}(u_{m'}(t) - u_m(t)) \qquad (3)$$

where $G = E/2(1+\nu)$, $\kappa = 3 - 4\nu$, and ν is Poisson's ratio. The results are plotted in Fig.7. Number of curve indicates the crack number in Fig.6 (b).

It is a matter of course that variation of SIF K_I is similar to that of crack opening angle. K_Is in the middle height of dam are high during cold season, about a quarter of

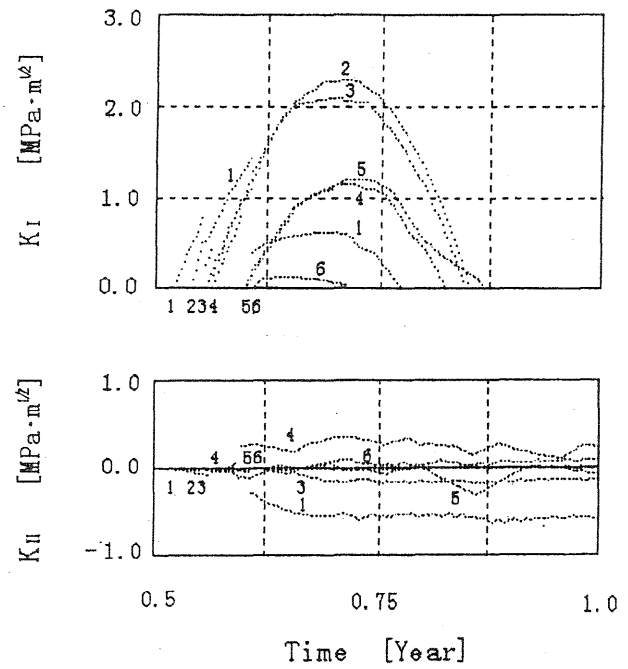

Fig.7 Time-stress intensity factor curve

one year, in comparison of the toughness K_{IC} of concrete obtained by usual material test. The highest value is 2.33 MPa · $m^{1/2}$ at crack 2 in the middle height. Curves of K_Is break and/or disappear after the onset of contact of the nodes pair. The earliest contact can be seen at crack 6.

Values of K_{II}s are overall low. Note that signs of K_{II}s depend upon the direction of shear forces. The highest absolute value of K_{II} is 0.59 MPa · $m^{1/2}$ at crack 1. K_{II}s of the upper and lower parts of dam are higher than those of the middle part. Sliding of the nodes pair develops, even under the condition of the contact. In Fig.7 variations of K_{II}s to the end of year are shown.

4 Conclusion

The discrete crack model and nodal forces release technique used in this study gave distinctive results on temporal and spatial occurrence and behavior of thermal cracks in a typical gravity dam. The used finite element mesh was not so dense. However, remarkable results were obtained that firstly the thermal cracks concentrated in the lower and upper parts of dam, and secondly the stress intensity factor K_I at the

thermal crack tip in the middle height of dam was high and the high value lasted relatively long period.

The adopted assumptions are not all based upon the real data. For further discussion, therefore, the validity of the results should be examined closely with reference to actual field observations.

5 References

Bangash, M.Y.H. (1989) **Concrete and Concrete Structures Numerical Modelling and Applications.** Elsevier, London and New York.

Higashigawa, T., Noike, E. and Yamakawa, S. (1992) Reduction of thermal stress and application of layer construction method in a hollow gravity dam (in Japanese). **Erectric Power Civil Engineering**, 242, 90-98.

Noike, E., Yamakawa, S. and Kawaraba, H. (1994) Thermal stress in concrete dam affected by natural cooling of reservoir water (in Japanese). **Electric Power Civil Engineering**, 253, 22-29.

Okubo, R., Ideguchi, H., Hara, T. and Jikan, S. (1989) Measurement analyses of thermal cracks in dam concrete structures (in Japanese). **Large dams**, 130, 1-10.

Scordelis, A.C., Ngo, D. and Franklin, H.A. (1974) Finite element study of reinforced concrete beams with diagonal tension in cracks, in **Shear Reinforced Concrete**, ACI Publ., SP-42, 79-102.

Shimizu, S. and Takahi, K. (1989) Study of time-dependent properties of surface cracking on mass concrete (in Japanese). **Large Dams**, 130, 24-29.